An Analysis of Liao's Absorbing Boundary Condition[†]

Robert L. Wagner and Weng Cho Chew
Electromagnetics Laboratory
Department of Electrical and Computer Engineering
University of Illinois
Urbana, IL 61801

Corresponding Author:
Weng Cho Chew
Electromagnetics Laboratory
Department of Electrical and Computer Engineering
University of Illinois
Urbana, IL 61801

[†]This work was supported by the Office of Naval Research under grant N00014-89-J-1296, by the Army Research Office under contract DAAH04-93-G-0430, and by the National Science Foundation under grant NSF-ECS-92-24466.

File: jewa_rev.tex 11/20/94

ABSTRACT

A theoretical and numerical analysis of Liao's absorbing boundary condition (ABC) is presented. The form of the ABC is related to both space-time polynomial extrapolation and a one-way wave equation. A modification allowing the optimization of the ABC for specific angles of incidence or wave speeds is discussed. The stability of the ABC is also discussed, and a technique is presented for enhancing stability. Numerical results are presented to demonstrate the stability and accuracy of the ABC.

I. INTRODUCTION

In this paper, we present a theoretical and numerical analysis of Liao's absorbing boundary condition (ABC) [1-4] for the termination of finite-difference time-domain computational grids. Liao's ABC has been used successfully by several researchers, for example in [5-7]. One advantage of Liao's ABC over some others is that, because of its form, it is easy to implement even near the corners of a computational grid. Here we offer some observations about the form of the ABC, and discuss some techniques for enhancing its stability and accuracy. First, the form of the ABC is examined, and related to both space-time polynomial extrapolation and a one-way wave equation. A modification allowing the ABC to be optimized for specific angles of incidence or wave speeds, briefly introduced in [3], is discussed. Also, the stability of the ABC is examined in some detail. The present discussion of stability extends that in [4], and relates the stabilization scheme presented there to the introduction of a damping factor in the one-way wave equation. Numerical results are presented to demonstrate the stability and accuracy of the ABC.

II. DESCRIPTION OF BOUNDARY CONDITION

The use of the finite-difference time-domain method is well known for the solution of the wave equation

$$\left(\frac{\partial^2}{\partial x^2}+\frac{\partial^2}{\partial y^2}-\frac{1}{c^2}\frac{\partial^2}{\partial t^2}\right)\phi(x,y;t)=0. \tag{1}$$

The scalar field ϕ is computed on a rectangular finite-difference grid with grid spacing $\triangle s$ and time step $\triangle t$: $\phi(m\triangle s, n\triangle s; l\triangle t)=\phi^l_{m,n}$. Using central differencing in time and space, the wave equation is approximated as

$$\frac{\phi^l_{m+1,n}-2\phi^l_{m,n}+\phi^l_{m-1,n}}{\triangle s^2}+\frac{\phi^l_{m,n+1}-2\phi^l_{m,n}+\phi^l_{m,n-1}}{\triangle s^2}-\frac{1}{c^2}\frac{\phi^{l+1}_{m,n}-2\phi^l_{m,n}+\phi^{l-1}_{m,n}}{\triangle t^2}=0. \tag{2}$$

At the boundaries of the finite computational domain, an absorbing boundary condition may be used to simulate radiation in an unbounded space.

For a "right" boundary at $x=x_0$, Liao's ABC gives the updated boundary field $\phi(x_0,y_0;t_0+\triangle t)$ in terms of field values at previous times lying along a straight line perpendicular to the boundary [1,2]:

$$\phi(x_0, y_0; t_0 + \triangle t) = \sum_{j=1}^{N} (-1)^{j+1} C_j^N \phi(x_0 - jc\triangle t, y_0; t_0 - (j-1)\triangle t), \tag{3}$$

where C_j^N is the binomial coefficient $N!/[j!(N-j)!]$ and N is the order of the boundary condition.

The boundary condition may be written in a simpler form by introducing the following operators:

$$\mathcal{Z}_t \phi(x, y; t) = \phi(x, y; t + \triangle t), \tag{4}$$

$$\mathcal{Z}_x \phi(x, y; t) = \phi(x + \triangle s, y; t), \tag{5}$$

$$\mathcal{A}\phi(x, y; t) = (T_{11} + T_{12}\mathcal{Z}_x^{-1} + T_{13}\mathcal{Z}_x^{-2})\phi(x, y; t) \approx \phi(x - c\triangle t, y; t). \tag{6}$$

The operators $\mathcal{Z}_t$ and $\mathcal{Z}_x$ are, respectively, forward time and space shifts. The operators $\mathcal{Z}_t^{-1}$ and $\mathcal{Z}_x^{-1}$ represent backward time and space shifts. The operator $\mathcal{A}$ approximates a backward spatial shift of $c\triangle t$ using quadratic interpolation, with interpolation coefficients

$$T_{11} = \frac{(2-s)(1-s)}{2}, \tag{7a}$$

$$T_{12} = s(2-s), \tag{7b}$$

$$T_{13} = \frac{s(s-1)}{2}, \tag{7c}$$

$$s = c\triangle t/\triangle s. \tag{7d}$$

Interpolation is necessary in $\mathcal{A}$ because field values are only available at grid points with spacing $\triangle s$, and in general $c\triangle t \neq \triangle s$. Using these operators and some algebraic manipulation of Equation (3), Liao's boundary condition may be rewritten as

$$\phi(x_0, y_0; t_0 + \triangle t) = [1 - (1 - \mathcal{A}\mathcal{Z}_t^{-1})^N]\mathcal{Z}_t \phi(x_0, y_0; t_0), \tag{8}$$

or, equivalently,

$$[1 - \mathcal{A}\mathcal{Z}_t^{-1}]^N \phi(x_0, y_0; t_0 + \triangle t) = 0. \tag{9}$$

It is readily seen that Liao's boundary condition is an example of what Higdon [8] refers to as a "space-time extrapolation" boundary condition. Suppose that a plane wave is normally incident on the boundary at (x_0, y_0), from the left, with velocity c. Then $\phi(x, y_0; t) = f(x - ct)$, and $\phi(x_0, y_0; t_0 + \triangle t) = f(x_0 - ct_0 - c\triangle t) = \phi(x_0 - c\triangle t, y_0; t_0)$. Thus, the behavior of the field at $(x_0, y_0; t_0 + \triangle t)$ may be extrapolated from knowledge of the field at the space-time point $(x_0 - c\triangle t, y_0; t_0)$. The operators $\mathcal{A}$ and $\mathcal{Z}_t^{-1}$ should cancel one another, rendering Equation (9) true. More generally, the incident wave may be composed of plane waves traveling at different angles to the x axis. Since a plane wave traveling with angle θ_i to the x axis has apparent velocity $c/\cos\theta_i$ in the x direction, the total field may be approximated as ([1,2]):

$$\phi(x, y_0; t) = \sum_i u_i(x - \frac{c}{\cos\theta_i} t). \tag{10}$$

In this case the field is no longer constant along space-time lines $[x - ct = \text{const}]$, but may be slowly varying along these lines, especially for small values of θ_i. The field $\phi(x_0, y_0; t_0 + \triangle t)$ may then be approximated by performing a polynomial extrapolation on the discrete field values $\phi(x_0 - c\triangle t, y_0; t_0), \phi(x_0 - 2c\triangle t, y_0; t_0 - \triangle t), \phi(x_0 - 3c\triangle t, y_0; t_0 - 2\triangle t), \ldots, \phi(x_0 - Nc\triangle t, y_0; t_0 - (N-1)\triangle t)$, which lie along the space-time line $[x - ct = x_0 - c(t_0 + \triangle t)]$.

To make use of this idea, we need a formula for polynomial extrapolation on a uniform grid. This may be obtained as a special case of the general Lagrange interpolation formula. Given N points x_j, $j = 1, 2, \ldots, N$, and corresponding function values $f_1, f_2, \ldots, f_N$, the unique polynomial of degree $N-1$ which matches the N function values above is given by the formula ([9], p. 878)

$$f(x) = \sum_{j=1}^{N} \frac{(x - x_1)\cdots(x - x_{j-1})(x - x_{j+1})\cdots(x - x_N)}{(x_j - x_1)\cdots(x_j - x_{j-1})(x_j - x_{j+1})\cdots(x_j - x_N)}\; f_j. \tag{11}$$

Specializing to the case of uniformly spaced samples $x_j = j\triangle, j = 1, 2, \ldots, N$, and evaluating at the point $x = x_0 = 0$, the above formula becomes

$$\begin{aligned} f_0 &\approx \sum_{j=1}^{N} \frac{\prod_{k=1}^{N}(x_0 - x_k)\cdot \frac{1}{(x_0 - x_j)}}{\prod_{k=1}^{j-1}(x_j - x_k)\cdot \prod_{k=j+1}^{N}(x_j - x_k)}\; f_j \\ &= \sum_{j=1}^{N} (-1)^{j+1} \frac{\left[\prod_{k=1}^{N} k\right]\cdot \frac{1}{j}}{[(j-1)(j-2)\cdots(1)]\cdot[(1)(2)\cdots(N-j)]}\; f_j \\ &= \sum_{j=1}^{N} (-1)^{j+1} \frac{N!}{j!(N-j)!}\; f_j = \sum_{j=1}^{N} (-1)^{j+1} C_j^N\; f_j. \end{aligned} \tag{12}$$

Applying this to the data $f_j = \phi(x_0 - jc\triangle t, y_0; t_0 - (j-1)\triangle t), j = 1, \ldots, N$, and evaluating at the point $(x_0, y_0; t_0 + \triangle t)$ (i.e. at $j = 0$) yields Equation (3). Thus, Liao's boundary condition of order N corresponds to space-time extrapolation with a polynomial of degree $(N-1)$.

Alternatively, as noted by Higdon [8], such a boundary condition can be seen to be consistent with the analytical boundary condition

$$\left(\frac{\partial}{\partial t} + c\frac{\partial}{\partial x}\right)^N \phi(x, y; t) = 0. \tag{13}$$

This may be seen by considering $N = 1$ in Equation (9):

$$[1 - \mathcal{A}\mathcal{Z}_t^{-1}]\phi(x, y; t) = 0. \tag{14}$$

Adding and subtracting $\mathcal{Z}_t^{-1}$ and multiplying both sides by $\mathcal{Z}_t/\triangle t$ yields

$$\left[\frac{(\mathcal{Z}_t - 1)}{\triangle t} + c\frac{(1 - \mathcal{A})}{c\triangle t}\right]\phi(x, y; t) = 0. \tag{15}$$

This is a "forward Euler" approximation to one of the terms in Equation (13): the first term represents a forward difference approximation to $\frac{\partial}{\partial t}$, and the second represents a backward difference approximation to $\frac{\partial}{\partial x}$ (recall that $\mathcal{A}$ approximates a backward spatial shift of $c\triangle t$).

Finally, we note that Liao's ABC may be optimized for the absorption of waves at incidence angles θ_i, $i = 1, 2, \ldots, N$, by modifying Equation (9) to be

$$\left[\prod_{i=1}^{N}\left(1 - \mathcal{A}(c_i)\mathcal{Z}_t^{-1}\right)\right]\phi(x_0, y_0; t_0 + \triangle t) = 0, \tag{16}$$

where $c_i = c/\cos\theta_i$. The dependence of $\mathcal{A}(c_i)$ on c_i is through the interpolation coefficients T_{11}, T_{12}, and T_{13} (Equations (6) and (7)). This modification was first introduced in [3], and bears close resemblance to Higdon's ABC [10]. Both Higdon's ABC and the above boundary condition are consistent with the analytical absorbing boundary condition

$$\left[\prod_{i=1}^{N}\left(\frac{\partial}{\partial t} + \frac{c}{\cos\theta_i}\frac{\partial}{\partial x}\right)\right]\phi(x, y; t) = 0. \tag{17}$$

In addition, both Higdon's and the modified Liao's boundary condition use only a one dimensional spatial stencil: they require only field data on a straight line perpendicular to the absorbing boundary. This makes these boundary conditions easy to implement near the corners of a computational grid. The difference between the two is in the finite-difference approximation to Equation (17). In addition to optimizing for specific angles of incidence, the above boundary condition may be viewed as a dispersive boundary condition, useful for absorbing frequency dispersive waves such as those found in a waveguide [11,12].

III. REFLECTION COEFFICIENT

Here we find the reflection coefficient of Liao's boundary condition for a discrete plane wave

$$\phi^l_{m,n} = e^{i(k_x m\triangle s + k_y n\triangle s - \omega l\triangle t)}. \tag{18}$$

The relationship between k_x, k_y, and ω is found by inserting the discrete plane wave above into the discrete wave equation (Equation (2)), yielding the dispersion relation

$$\sin^2\left(\frac{k_x\triangle s}{2}\right) + \sin^2\left(\frac{k_y\triangle s}{2}\right) = \left(\frac{\triangle s}{c\triangle t}\right)^2 \sin^2\left(\frac{\omega\triangle t}{2}\right). \tag{19}$$

An extensive discussion of this dispersion relation is given in [8] and [10]. An excellent general discussion of dispersion relations and group velocity is given in [13]. Here we simply note that for a fixed k_y and ω there are two solutions for k_x in Equation (19), one right-going and one left-going. Denoting the right-going solution as k_{xr} and the left-going solution as k_{xl}, the total plane wave field to the left of a reflecting boundary may be written

$$\phi^l_{m,n} = e^{i(k_y n\triangle s - \omega l\triangle t)}\left(e^{ik_{xr}m\triangle s} + Re^{ik_{xl}m\triangle s}\right) = \phi_{\text{inc}} + R\phi_{\text{ref}}, \tag{20}$$

where R is the reflection coefficient for the boundary. The geometry is shown in Figure 1. For purely oscillatory waves with k_x, k_y, and ω all real, the wave is right-going (both phase and group velocity greater than or equal to zero) if k_x and ω have the same sign. When k_x and ω have opposite signs, the wave is left-going. For such purely oscillatory waves, $k_{xl} = -k_{xr}$.

To determine the reflection coefficient for the generalized Liao's boundary condition, apply the boundary operator of Equation (16) to the field of Equation (20), and solve for R. Note that when the operators $\mathcal{Z}_t$, $\mathcal{Z}_x$, and $\mathcal{A}$ are applied to the discrete plane wave of Equation (18), they become scalars as follows:

$$\mathcal{Z}_t \to z_t \equiv e^{-i\omega\triangle t}, \tag{21a}$$

$$\mathcal{Z}_x \to z_x \equiv e^{ik_x\triangle s}, \tag{21b}$$

$$\mathcal{A} \to \mathcal{A}(c, z_x) \equiv T_{11} + T_{12} z_x^{-1} + T_{13} z_x^{-2}. \tag{21c}$$

Using this notation, the total field becomes

$$\phi_{m,n}^l = e^{ik_y n\triangle s} z_t^l \left(z_{xr}^m + R z_{xl}^m\right), \tag{22}$$

and the reflection coefficient for the generalized Liao's ABC is found to be

$$R = -\prod_{i=1}^{N} \left(\frac{1 - \mathcal{A}(c_i, z_{xr}) \cdot z_t^{-1}}{1 - \mathcal{A}(c_i, z_{xl}) \cdot z_t^{-1}} \right). \tag{23}$$

Figure 2 shows the theoretical reflection coefficient for the original Liao's ABC for orders $N = 3$ and $N = 5$, the modified Liao's ABC for order $N = 3$ and optimization angles $\{\theta_1 = 10°, \theta_2 = 30°, \theta_3 = 42°\}$, and the widely used second order Mur ABC [14]. The Liao reflection coefficients are calculated using Equation (23) and the discrete dispersion relation of Equation (19), with discretization $c\triangle t/\triangle s = 0.5$ and $\omega\triangle t = 0.05$. The Mur reflection coefficient is calculated in a similar manner, using the appropriate boundary operator from [14], and with the same discretization.

IV. STABILITY

The general theory of the stability of finite-difference equations with absorbing boundaries is a rather complicated topic, and has been much discussed in the mathematical literature [8,10,13,15,16]. The fundamental result is the stability theory of Gustafsson, Kreiss, and Sundström [15], which gives the stability criterion for Liao's ABC as [10]

$$1 - \mathcal{A}(c_i, z_{xl}) \cdot z_t^{-1} \neq 0 \text{ whenever} |z_t| \geq 1, \text{ for all } k_y\triangle s. \tag{24}$$

That is, the reflection coefficient R (Equation (23)) should not have any poles on or outside the unit circle in the complex z_t-plane. Note that it is sufficient to consider real $k_y\triangle s$ in the range $[-\pi, \pi]$, as this allows for the representation of arbitrary y-dependence through a Fourier transform.

Some clarification is necessary in Equation (24) regarding the definition of z_{xl} when $|z_t| > 1$. For discussion of this, it is helpful to rewrite the dispersion relation (Equation (19)) in terms of $z_t \equiv e^{-i\omega\triangle t}$ and $z_x \equiv e^{ik_x\triangle s}$. Inserting the discrete plane wave $\phi^l_{m,n} = e^{ik_y n\triangle s} z_t^l z_x^m$ into the discrete wave equation (Equation (2)) yields an alternative form for the dispersion relation

$$(z_x - 2 + z_x^{-1}) + (e^{ik_y\triangle s} - 2 + e^{-ik_y\triangle s}) = \left(\frac{\triangle s}{c\triangle t}\right)^2 (z_t - 2 + z_t^{-1}). \qquad (25)$$

From this form, it can be seen that, for fixed z_t and k_y, there are two solutions for z_x: z_{x1} and z_{x2}. Furthermore, from the symmetry of z_x and z_x^{-1} above, the two solutions must be reciprocals of one another: $z_{x2} = 1/z_{x1}$.

Previously, we discussed the classification of the two solutions for z_x as right-going and left-going waves, when $|z_x| = |z_t| = 1$. As discussed in [10], this classification may be extended to the case $|z_t| > 1$ by choosing z_{xr} and z_{xl} such that $|z_{xr}| < 1$ and $|z_{xl}| > 1$. That is, when $|z_t| > 1$, the waves decay in their direction of propagation. Furthermore, z_{xr} and z_{xl} defined in this manner smoothly approach the previous definition of z_{xr} and z_{xl} (in terms of right-going and left-going solutions) as $|z_t| \to 1$ and $|z_x| \to 1$ [10]. Also, when $k_y \neq 0$, there may be evanescent waves with $|z_t| = 1$, $|z_{xr}| < 1$, and $|z_{xl}| > 1$. Thus, it is clear what is meant by z_{xr} and z_{xl} for all $|z_t| \geq 1$. The reader is referred to the detailed discussion in [10] for more information.

With this classification in mind, a physical interpretation of the stability condition above is that there should be no inward travelling waves which satisfy the boundary condition and the interior difference equation, and which do not decay exponentially with time. That is, the finite-difference scheme with boundary conditions should not allow numerical noise at the boundary to excite a spurious, growing solution, which radiates energy from the boundary into the interior of the computational grid. This interpretation is developed extensively by Trefethen [13,16].

If Equation (24) admits a solution with $|z_t| > 1$ the numerical scheme is clearly unstable: there will be a spurious solution which grows exponentially with time, eventually swamping the desired solution to the wave equation. For the case where the poles of the reflection coefficient are located on the unit circle, the stability of the numerical scheme is marginal. Solutions to Equation (24) with $|z_t| = |z_{xl}| = 1$ are called *generalized eigensolutions* [13].

Thus, the stability of Liao's ABC depends on the locations, in the complex z_t-plane, of the simultaneous solutions to Equations (24) and (25). For identifying solutions, it is helpful to expand $\mathcal{A}$ in Equation (24) and rearrange to get the pole condition

$$z_t - T_{11} - T_{12} z_{xl}^{-1} - T_{13} z_{xl}^{-2} = 0. \tag{26}$$

It is readily seen that there is a potential problem when $k_y \triangle s = 0$ and $z_t = 1$. In this case, the dispersion relation has a double root: $z_{xr} = z_{xl} = 1$. Then the left-hand-side in Equation (26) becomes $1 - T_{11} - T_{12} - T_{13}$, which is found to be zero upon inserting the definitions for the interpolation coefficients T_{1i} given in Equation (7). Thus, the reflection coefficient R has a marginally stable pole at $z_t = 1$ (i.e. at frequency $\omega = 0$). Furthermore, if the interpolation coefficients T_{1i} are perturbed from their theoretical values by the limitations of machine precision, this pole may be shifted outside the unit circle, producing a catastrophic instability in the finite-difference scheme. Such instability has been observed for single-precision calculations with Liao's ABC of order $N = 3$ [4], and for double precision calculations with Liao's ABC of order $N \geq 5$ (Section V).

The effects of perturbing the coefficients T_{1i} were investigated previously in [4]. There, such perturbations were considered as a means for stabilizing Liao's ABC when using single-precision arithmetic. It was found that adding small negative numbers d_1, d_2, and d_3 to T_{11}, T_{12}, and T_{13}, respectively, stabilized the originally unstable single-precision ABC.

This is consistent with Figures 3 and 4, which show the effects of perturbing T_{11} by an amount $d_1 = \pm 0.025$. These are plots of $1/|z_t - T_{11} - T_{12} z_{xl}^{-1} - T_{13} z_{xl}^{-2}|$, in the complex ω-plane, with $k_y = 0$. Since $z_t \equiv e^{-i\omega\triangle t}$, the region $\Im m[\omega] > 0$ corresponds to $|z_t| > 1$. In Figure 3, the perturbation is $d_1 = +0.025$ and an unstable pole of R is clearly visible in the region $\Im m[\omega] > 0$. In Figure 4, it is seen that with $d_1 = -0.025$, the pole is pushed safely out of $\Im m[\omega] > 0$, or inside the unit circle on the complex z_t-plane. This behavior is summarized in Figure 5, which illustrates qualitatively the motion of the pole of R in the complex z_t-plane, as the perturbation d_1 is varied. Similar behavior was observed for perturbations d_2 and d_3: positive values push the pole outside the unit circle (unstable), and negative values push the pole inside the unit circle (stable).

It is interesting to note that a perturbation of T_{11} is identical to a stabilization scheme suggested by Higdon [10], Betz and Mittra [12], and Fang [17]. The suggested remedy is the addition of a small damping term α to the one way wave equation, modifying Equation (17) to be

$$\left[\prod_{i=1}^{N}\left(\frac{\partial}{\partial t}+\frac{c}{\cos\theta_i}\frac{\partial}{\partial x}+\alpha_i\right)\right]\phi(x,y;t)=0. \tag{27}$$

Examining Equation (15), it is seen that a perturbation of T_{11} by an amount $-\delta$ (i.e. $d_1 = -\delta$) is equivalent to adding a positive damping term $\alpha = \delta/\triangle t$ to the one way wave equation.

The damping effect of α may be explained as follows [12]. Suppose a wave $f(x,y;t)$ satisfies $(\frac{\partial}{\partial t}+c\frac{\partial}{\partial x})f(x,y;t)=0$. Then a quick check shows that the function $f(x,y;t)e^{-\alpha t}$ satisfies $(\frac{\partial}{\partial t}+c\frac{\partial}{\partial x}+\alpha)f(x,y;t)e^{-\alpha t}=0$. So, if $f(x,y;t)$ represents a marginally stable inward travelling solution to the interior finite-difference equation and original boundary condition, the addition of small positive terms α_i as in Equation (27) forces the unwanted solution to decay exponentially, rendering the numerical model stable. This is equivalent to shifting the marginally stable poles of R inside the unit circle in the complex z_t-plane. We note that this stabilization scheme applies to both single- and double-precision calculations: in either case, the effect will be to shift the poles of R inside the unit circle.

As a guideline for choosing the value of δ, we note that Fang [17] uses a damping coefficient $\alpha = 0.04c/\triangle s$, while Betz and Mittra [12] state that any value of α between $0.05c/\triangle s$ and $0.3c/\triangle s$ yields reasonable results. This suggests that a good choice for δ would be in the range $0.04c\triangle t/\triangle s$ to $0.3c\triangle t/\triangle s$. This is confirmed by the results of our numerical simulations.

V. NUMERICAL RESULTS

Here we present some numerical simulations to demonstrate the stability and accuracy of Liao's ABC. The simulations were carried out using a 2-D Yee algorithm for a TM (E_z) wave in free space excited by a line source J_z. All computations were performed on a SPARC workstation in double-precision arithmetic. The computational grid for boundary condition tests was 50 cells on a side, with grid parameters $\triangle s = 0.01$m and $\triangle t = 1.67\times 10^{-11}$sec, so that $c\triangle t/\triangle s = 0.5$. This satisfies the

CFL stability criterion $c\triangle t/\triangle s < 1/\sqrt{2}$ [2]. The line source had time dependence [5] $J_z(t) = \left[4(t/\tau)^3 - (t/\tau)^4\right] e^{-t/\tau}/\triangle s^2$, with time constant $\tau = 1.64 \times 10^{-10}$sec, and was located at the center of the grid. The absorbing boundary conditions were applied to E_z on all four computational boundaries. To study the accuracy of the ABCs, a reference solution was also computed with the source at the center of a similar but larger grid (550 cells on a side), so any boundary reflections could be time gated out in a 50 cell by 50 cell square region around the source.

The stability of the third order Liao's ABC under perturbations of the interpolation coefficient T_{11} is demonstrated in Figure 6. Shown is the computed solution for the electric field, at a receiver located ten grid points to the right of the line source. In the third order Liao's ABC, only one of the three T_{11}'s was perturbed; the other two were unchanged. The results are in agreement with the stability theory of Section IV: positive perturbations of T_{11} render the boundary condition unstable, and negative perturbations enhance stability.

Also plotted in Figure 6 is the reference solution, which is seen to be in good agreement with the result obtained using the stabilized ABC. While the results here are computed using double-precision arithmetic, good results have also been demonstrated for single-precision calculations, using the stabilized third order ABC [4]. As an example of the application of the third order Liao's ABC to a practical problem, we note that this boundary condition was successfully used in [5] to model a subsurface interface radar.

The accuracy of the boundary condition is studied further by computing the norm of the error field that is reflected back into the computational grid because of the imperfect absorbing boundaries. The error field norm is defined as

$$\mathrm{ERR}^l = \frac{\sqrt{\sum_{m=6}^{45}\sum_{n=6}^{45}\left[E^l_{z\ m,n} - E^{l\ \mathrm{ref}}_{z\ m,n}\right]^2}}{\max\limits_j \sqrt{\sum_{m=6}^{45}\sum_{n=6}^{45}\left[E^{j\ \mathrm{ref}}_{z\ m,n}\right]^2}}, \tag{28}$$

where $E^{l\ \mathrm{ref}}_{z\ m,n}$ is the reference solution computed on a large grid. The first five cells near the boundary are not included in the error norm because the behavior of the field near the boundary is not usually of paramount importance. The significant factor is how much energy propagates back into the interior of the simulation region, where receivers or near-to-far-field transformation surfaces are located.

The error for the third and fifth order Liao's ABC is shown in Figures 7 and 8, respectively. Two versions of each boundary condition are included: one the original ABC, and one with perturbed values of T_{11}. For each of the N factors in Liao's ABC (Equation (9)), T_{11} was perturbed by an amount $-\delta_i$, corresponding to a damping factor of $\alpha_i = +\delta_i/\triangle t$ in Equation (27). Note that the unperturbed fifth order ABC was unstable, but was stabilized by the added damping terms. The perturbed results shown represent the best set of δ_i's found (by trial and error) for reducing the error norm and maintaining stability. For the third order boundary condition, the best result found was with $\{\delta_1 = \delta_2 = 0.0025, \delta_3 = 0.025\}$. For the fifth order boundary condition, the best result found was with $\{\delta_1 = \delta_2 = 0.0025, \delta_3 = \delta_4 = \delta_5 = 0.025\}$. The small perturbations δ_1 and δ_2 helped maintain late-time stability, and the other larger perturbations provided improved absorption, as seen in the figures. Note that the larger perturbations, $\delta = 0.025$, correspond to $\delta = 0.05c\triangle t/\triangle s$ (since $c\triangle t/\triangle s = 0.5$ here). Thus, these results are in agreement with the guidelines for choosing δ discussed at the end of Section IV.

The best results obtained here were achieved with the stabilized fifth order Liao's ABC. Attempts to find a stable and accurate seventh order Liao's ABC were unsuccessful. This may be due to the fact that Liao's ABC is equivalent to polynomial extrapolation, and high order polynomial interpolation/extrapolation is often badly behaved [18].

We note briefly that for this numerical test case the use of the modified Liao's ABC of Equation (16), allowing the optimization of the ABC for specific angles of incidence, had little effect on the solution error. We attempted to decrease the norm of the reflected field by distributing the nulls of the ABC in order to produce better wide-angle absorption. For example, we tried using the third order modified Liao's ABC with optimization angles $\{\theta_1 = 10°, \theta_2 = 30°, \theta_3 = 42°\}$. The theoretical reflection coefficient of this ABC is shown in Figure 2. However, using this ABC, as well as other sets of optimization angles (chosen by trial and error), did not significantly decrease the solution error when compared with the original Liao's ABC. This is consistent with the findings of [19], where it was observed that the optimization angles used in Higdon's ABC had little effect on performance when the absorbing boundary was in the near field of the source. In our test case, the boundaries are 25cm from the source, corresponding to 0.4 wavelengths at the center frequency of the source pulse ($f_c = 1/4\pi\tau = 485.2$MHz, $\lambda_c = c/f_c = 62$cm), making this a near-field boundary. It is expected that the modified ABC may still be useful as a dispersive boundary condition for waveguide termination, or for far-field absorption.

VI. CONCLUSIONS

In this paper, we have presented a theoretical and numerical analysis of Liao's absorbing boundary condition. We have made the following observations:

(1) The original Liao's ABC of order N (Equation (9)) is equivalent to space-time extrapolation with a polynomial of degree $(N-1)$.

(2) The generalized Liao's ABC of order N (Equation (16)) is consistent with the analytical boundary condition

$$\left[\prod_{i=1}^{N}\left(\frac{\partial}{\partial t}+\frac{c}{\cos\theta_i}\frac{\partial}{\partial x}+\alpha_i\right)\right]\phi(x,y;t)=0, \tag{29}$$

with $\alpha_i = 0$. The generalized ABC may be optimized for the absorption of waves at specific angles of incidence, θ_i, or specific velocities. This ABC is very similar to Higdon's, the difference being in the finite difference approximation to Equation (29). At the present time, we have not carried out a direct comparison of the accuracy and stability of Liao's and Higdon's ABCs. This would make an interesting topic for future work.

(3) The stability of the ABC depends on the locations in the complex z_t-plane ($z_t \equiv e^{-i\omega\triangle t}$) of the poles of the reflection coefficient R. The original ABC is marginally stable, with a pole on the unit circle in the z_t-plane. The boundary condition may be stabilized by adding damping terms α_i as in Equation (29). This may be achieved in practice by perturbing the interpolation coefficient T_{11} by an amount $-\delta$, producing a damping factor $\alpha = \delta/\triangle t$. This shifts the marginally stable pole of the reflection coefficient inside the unit circle, stabilizing the ABC.

(4) Use of damping factors α_i both stabilizes the ABC and improves the numerical performance. The best numerical results obtained here were achieved using a stabilized fifth order Liao's ABC. Attempts to produce a stable and accurate seventh order ABC were unsuccessful.

(5) For the generalized Liao's ABC, the numerical performance was not improved by adjusting the optimization angles θ_i. It is believed that this is because, in the numerical test used, the absorbing boundary was in the near field of the source.

REFERENCES

[1] Z.P. Liao, H.L. Wong, B.P. Yang, and Y.F. Yuan, "A transmitting boundary for transient wave analyses," *Scientia Sinica (Series A)*, vol. 27, no. 10, pp. 1063-1076, October 1984.

[2] W.C. Chew, *Waves and fields in inhomogeneous media.* New York: Van Nostrand Reinhold, 1990.

[3] W.C. Chew and R.L. Wagner, "A modified form of Liao's absorbing boundary condition," *IEEE AP-S/URSI Int. Symp. Dig.*, Chicago, IL, pp. 536-539, July 1992.

[4] M. Moghaddam and W.C. Chew, "Stabilizing Liao's absorbing boundary conditions using single-precision arithmetic," *IEEE AP-S/URSI Int. Symp. Dig.*, London, Ontario, Canada, pp. 430-433, June 1991.

[5] M. Moghaddam, E.J. Yannakakis, W.C. Chew, and C. Randall, "Modeling of the subsurface interface radar," *J. Electromag. Waves Appl.*, vol. 5, no. 1, pp. 17-39, 1991.

[6] S.R. Omick and S.P. Castillo, "A new finite-difference time-domain algorithm for the accurate modeling of wide-band electromagnetic phenomena," *IEEE Trans. Electromag. Compat.*, vol. 35, no. 2, May 1993.

[7] C.W. Penny and R.J. Luebbers, "Input impedance, radiation pattern, and radar cross section of spiral antennas using FDTD," *IEEE Trans. Ant. Prop.*, vol. 42, no. 9, pp. 1328-1332, September 1994.

[8] R.L. Higdon, "Absorbing boundary conditions for difference approximations to the multi-dimensional wave equation," *Math. Comp.*, vol. 47, no. 176, pp. 437-459, October 1986.

[9] M. Abramowitz and I.A. Stegun, "Handbook of mathematical functions," New York: Dover Publications, Inc., 1965.

[10] R.L. Higdon, "Numerical absorbing boundary conditions for the wave equation," *Math. Comp.*, vol. 49, no. 179, pp. 65-90, July 1987.

[11] Z. Bi, K. Wu, C. Wu, and J. Litva, "A dispersive boundary condition for microstrip component analysis using the FD-TD method," *IEEE Trans. Microwave Theory Tech.*, vol. 40, no. 4, pp. 774-777, April 1992.

[12] V. Betz and R. Mittra, "Comparison and evaluation of boundary conditions

for the absorption of guided waves in an FDTD simulation," *IEEE Microwave Guided Waves Lett.*, vol. 2, no. 12, pp. 499-501, December 1992.

[13] L.N. Trefethen, "Group velocity in finite difference schemes," *SIAM Review*, vol. 24, no. 2, pp. 113-136, April 1982.

[14] G. Mur, "Absorbing boundary condition for the finite-difference approximation of the time-domain electromagnetic-field equations," *IEEE Trans. Electromag. Compat.*, vol. 23, no. 4, pp. 377-382, November 1981.

[15] B. Gustafsson, H.-O. Kreiss, and A. Sundström, "Stability theory of difference approximations for initial boundary value problems II," *Math. Comp.*, vol. 26, pp. 649-686, 1972.

[16] L. N. Trefethen, "Instability of difference models for hyperbolic initial boundary value problems," *Comm. Pure Appl. Math*, vol. 37, pp. 329-367, 1984.

[17] J. Fang, "Investigation on the stability of absorbing boundary conditions for the time-domain finite-difference method," *IEEE AP-S/URSI Int. Symp. Dig.*, Chicago, IL, pp. 548-551, July 1992.

[18] W.H. Press, S.A. Teukolsky, W.T. Vetterling, and B.P Flannery, *Numerical recipes in Fortran: the art of scientific computing - 2nd ed.*, New York: Cambridge University Press, 1992.

[19] C.J. Railton and E.M. Daniel, "A comparison of the properties of radiating boundary conditions in the FDTD method for finite discretisation and non-planar waves," *IEEE Trans. Ant. Prop.*, vol. 42, no. 2, pp. 276-281, February 1994.

FIGURE CAPTIONS

Figure 1. Geometry of the absorbing boundary, showing the incident (right-going) and reflected (left-going) waves.

Figure 2. Theoretical reflection coefficient for the original Liao's ABC for orders $N = 3$ $(+)$ and $N = 5$ $(\diamond)$, the modified Liao's ABC for order $N = 3$ and optimization angles $\{\theta_1 = 10°, \theta_2 = 30°, \theta_3 = 42°\}$ $(\circ)$, and the second order Mur ABC $(\Box)$.

Figure 3. Plot of $1/|z_t - T_{11} - T_{12}z_{xl}^{-1} - T_{13}z_{xl}^{-2}|$, in the complex ω-plane, with $k_y = 0$. Here T_{11} is perturbed by an amount $d_1 = +0.025$, and the pole of R is driven into the unstable region $\Im m[\omega] > 0$.

Figure 4. Plot of $1/|z_t - T_{11} - T_{12}z_{xl}^{-1} - T_{13}z_{xl}^{-2}|$, in the complex ω-plane, with $k_y = 0$. Here T_{11} is perturbed by an amount $d_1 = -0.025$, and the pole of R is driven out of the unstable region $\Im m[\omega] > 0$.

Figure 5. Qualitative illustration of the motion of the pole of the reflection coefficient R, in the complex z_t-plane, under perturbation of the interpolation coefficient T_{11} by an amount d_1.

Figure 6. Electric field E_z at a receiver located ten grid points to the right of the line source, computed with a third order Liao's ABC with a single perturbed interpolation coefficient T_{11}: $T_{11} + 0.025$ $(+)$, $T_{11} - 0.025$ $(\times)$. Also shown is the reference solution $(\circ)$.

Figure 7. Norm over the computational grid of the reflection errors due to the following ABCs: third order Liao, unperturbed $(\circ)$, third order Liao, perturbed $(\Box)$.

Figure 8. Norm over the computational grid of the reflection errors due to the following ABCs: fifth order Liao, unperturbed $(\diamond)$, fifth order Liao, perturbed $(\triangle)$.

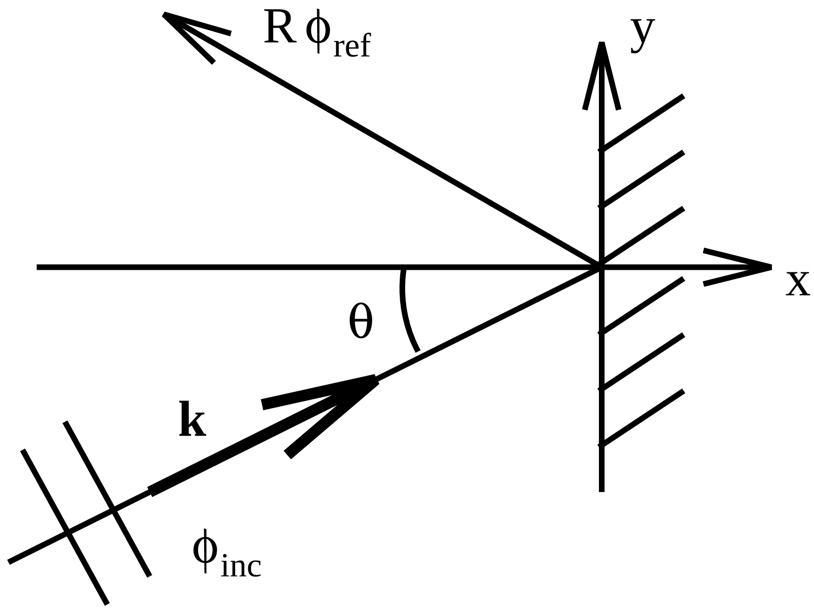

Figure 1. Geometry of the absorbing boundary, showing the incident (right-going) and reflected (left-going) waves.

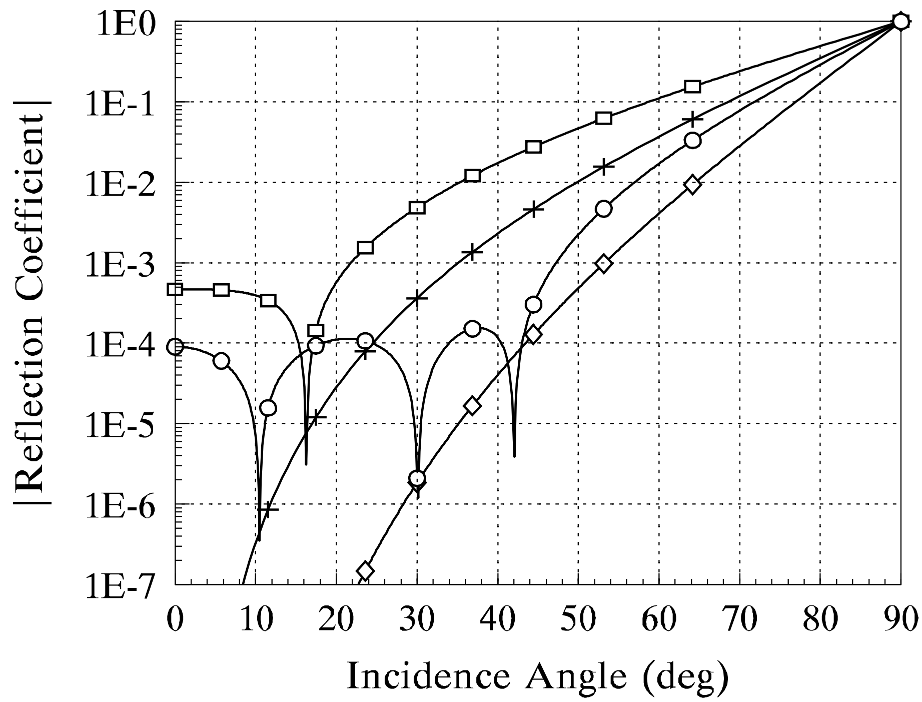

Figure 2. Theoretical reflection coefficient for the original Liao's ABC for orders $N = 3$ $(+)$ and $N = 5$ $(\diamond)$, the modified Liao's ABC for order $N = 3$ and optimization angles $\{\theta_1 = 10°, \theta_2 = 30°, \theta_3 = 42°\}$ $(\circ)$, and the second order Mur ABC $(\square)$.

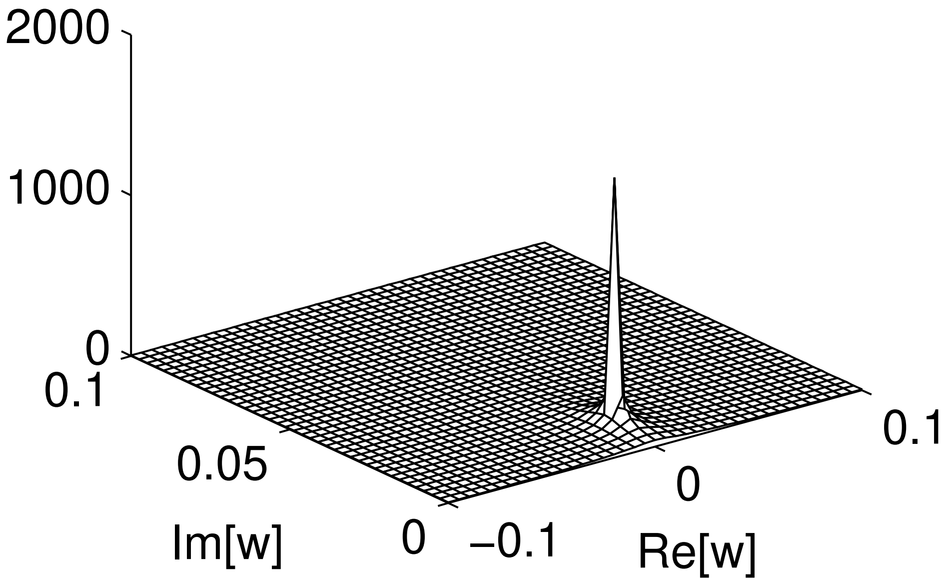

Figure 3. Plot of $1/|z_t - T_{11} - T_{12} z_{xl}^{-1} - T_{13} z_{xl}^{-2}|$, in the complex ω-plane, with $k_y = 0$. Here T_{11} is perturbed by an amount $d_1 = +0.025$, and the pole of R is driven into the unstable region $\Im m[\omega] > 0$.

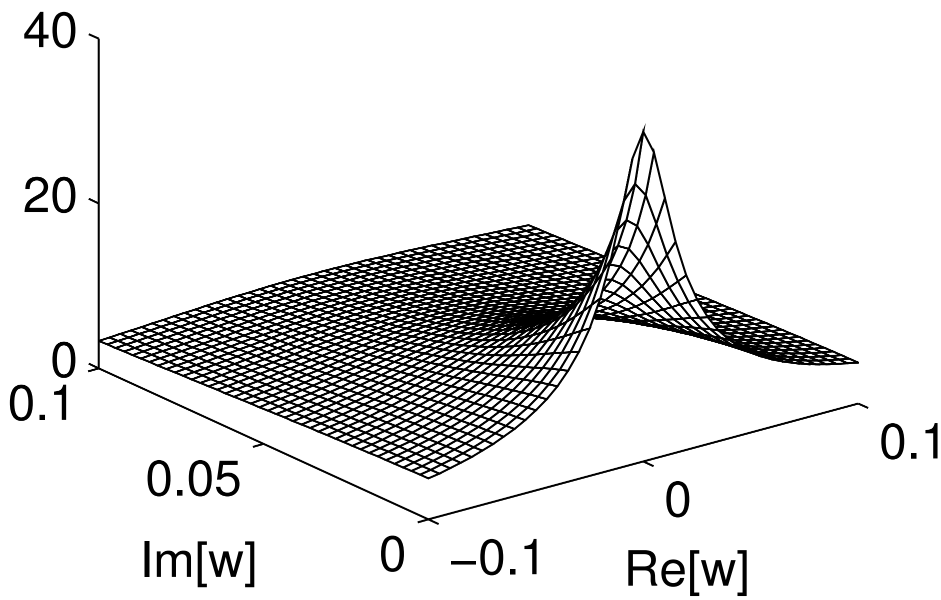

Figure 4. Plot of $1/|z_t - T_{11} - T_{12} z_{xl}^{-1} - T_{13} z_{xl}^{-2}|$, in the complex ω-plane, with $k_y = 0$. Here T_{11} is perturbed by an amount $d_1 = -0.025$, and the pole of R is driven out of the unstable region $\Im m[\omega] > 0$.

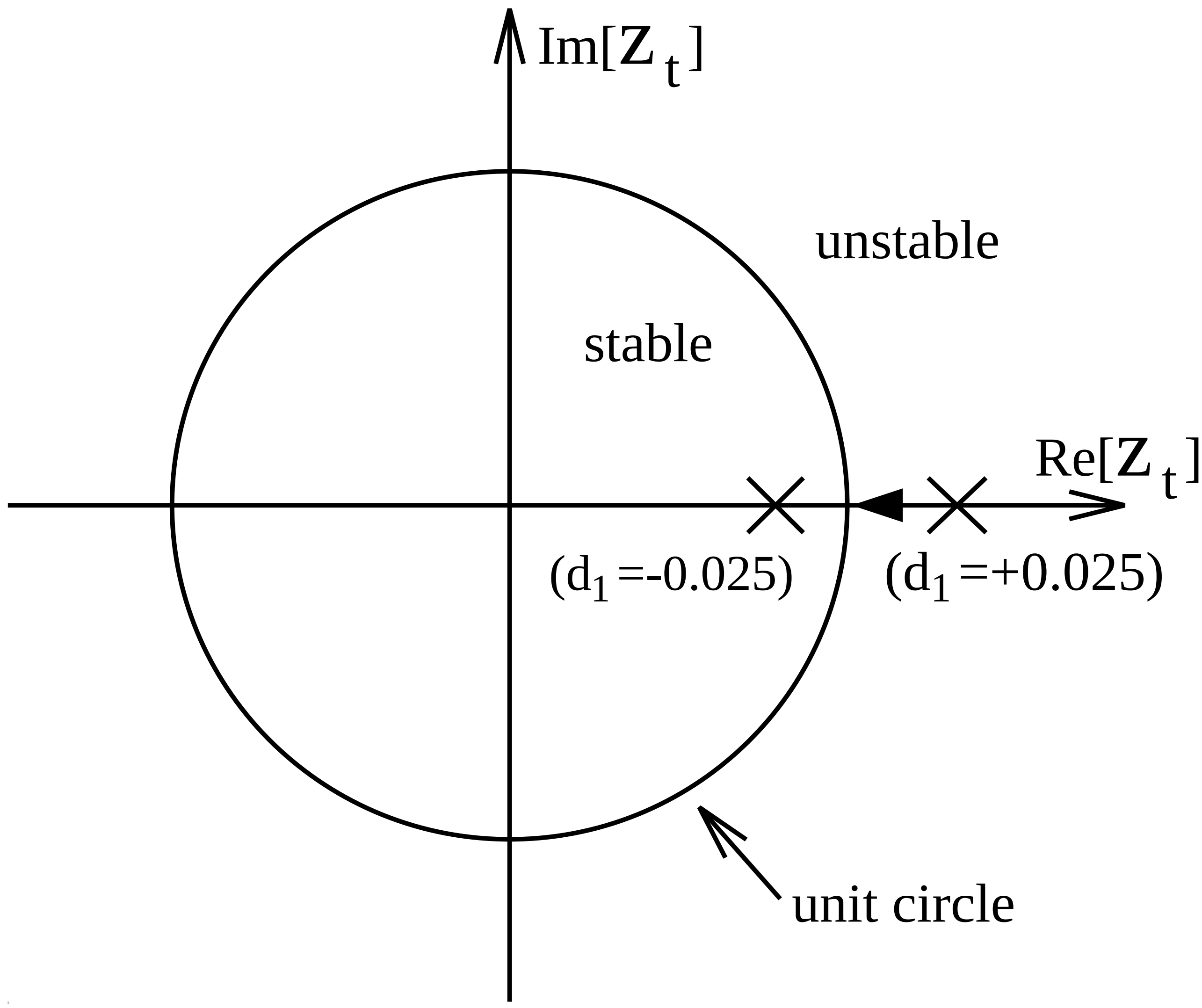

Figure 5. Qualitative illustration of the motion of the pole of the reflection coefficient R, in the complex z_t-plane, under perturbation of the interpolation coefficient T_{11} by an amount d_1.

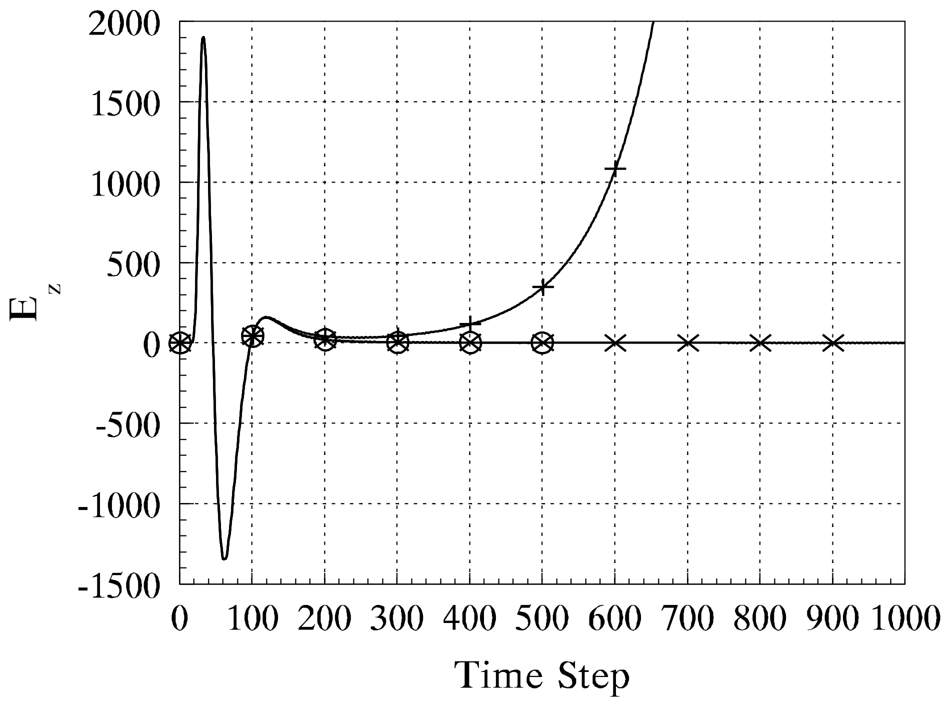

Figure 6. Electric field E_z at a receiver located ten grid points to the right of the line source, computed with a third order Liao's ABC with a single perturbed interpolation coefficient T_{11}: $T_{11} + 0.025$ $(+)$, $T_{11} - 0.025$ $(\times)$. Also shown is the reference solution $(\circ)$.

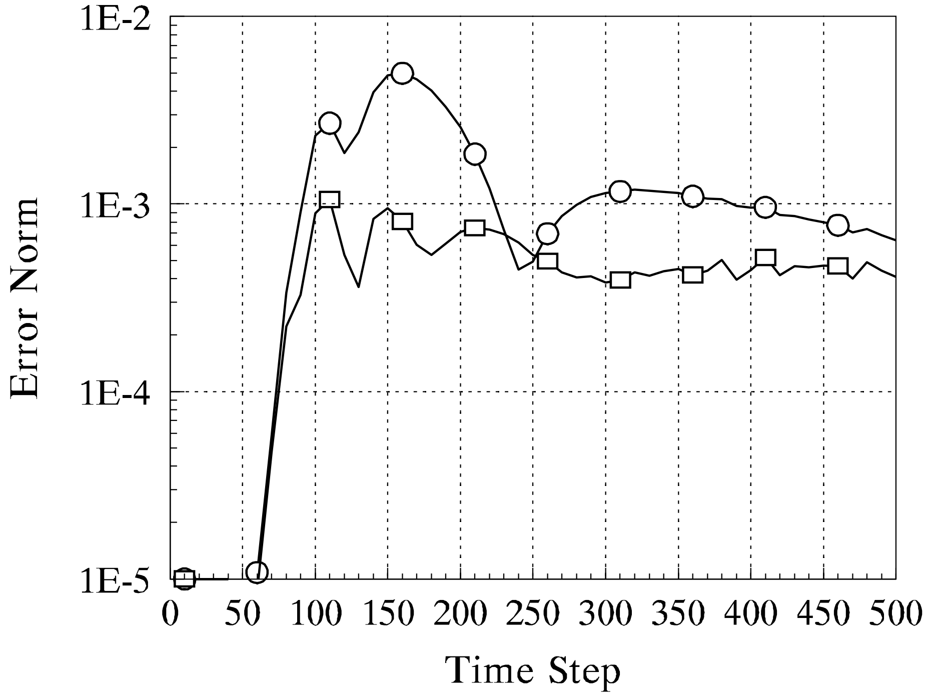

Figure 7. Norm over the computational grid of the reflection errors due to the following ABCs: third order Liao, unperturbed ($\circ$), third order Liao, perturbed ($\square$).

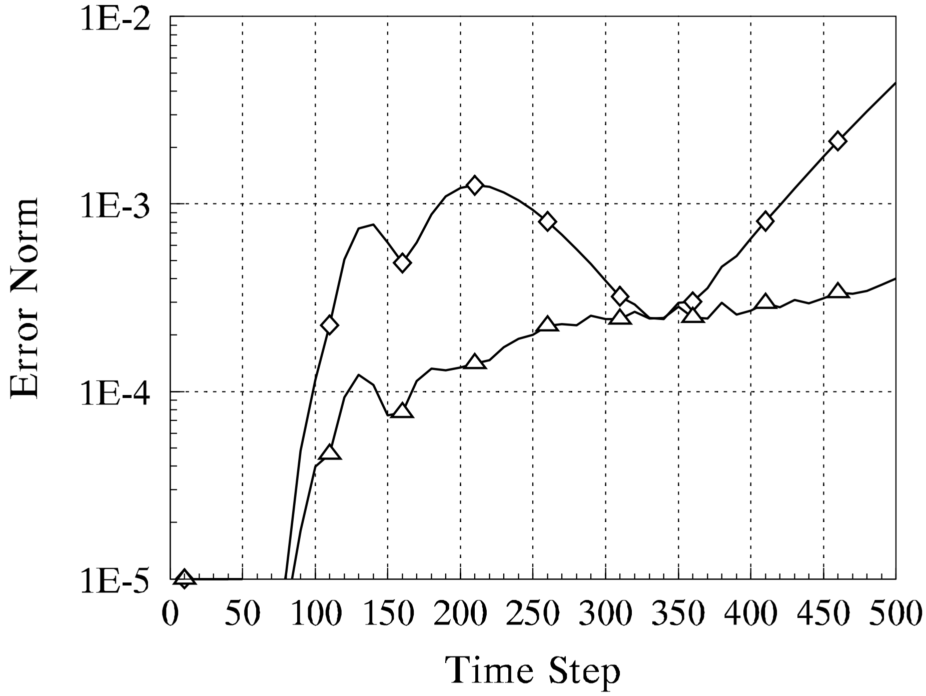

Figure 8. Norm over the computational grid of the reflection errors due to the following ABCs: fifth order Liao, unperturbed ($\diamond$), fifth order Liao, perturbed ($\triangle$).